

Effect of latitudinal displaced gravity wave forcing in the stratosphere on the circulation of the middle atmosphere

N. Samtleben¹, C. Jacobi¹, P. Šácha², P. Pišoft² and A. Kuchar²

Leipzig Institute for Meteorology, Universität Leipzig, Leipzig, Germany¹

Department of Atmospheric Physics, Charles University, Prague, Czech Republic²

Email: Nadja.Samtleben@uni-leipzig.de



Introduction

- Gravity waves (GWs) are the major contributor to vertical coupling of atmospheric layers by distributing energy and momentum throughout the whole atmosphere.
- GWs have horizontal wavelengths of tens to hundreds of kilometers so that GWs are mostly parameterized in global circulation models as zonal means.
- Breaking GW hotspots have been observed in the stratosphere [Šácha et al., 2015].
- Objective:** Effect of non-zonal GW distribution has to be analyzed.
- Hypothesis:** Preconditioning of the polar vortex by impact of GWs at midlatitudes [Albers and Birner, 2014].

MUAM – Middle and Upper Atmosphere Model

- Primitive equation 3D grid point model [Lilienthal et al., 2017; Samtleben et al., 2019]
- horizontal resolution: $5^\circ \times 5.625^\circ$
- Upper boundary: 160 km (log-p) with $\Delta z = 2.842$ km
- Nudging of ERA-Interim zonal mean temperature (decadal mean: 2000-2010) below 10 km
- GW parameterization: linear scheme with multiple breaking levels
- GW initialized at 10 km (1 cm s⁻¹ vertical velocity perturbation)



Fig. 1: Horizontal resolution of MUAM.

Model setup: Local non-zonal GW forcing

1. Gravity wave distribution in MUAM:

- Zonal mean GW distribution based on the observed potential energy (E_{pot}) data derived from GPS radio occultations (FORMOTSAT3/COSMIC)
- E_{pot} divided by its global mean E_{pot} at each grid point

2. Implementation of the non-zonal GW forcing:

- Artificial enhanced GW drag in the GW parameterization output (period of simulation: 120 days)
- Position of observed breaking GW hotspot: **Longitude:** 120-170°E
Latitude: 37.5-62.5°N
Height: 18-30km
- Latitudinal displacement of the GW hotspot in 5° steps (H1-H8) with a southernmost (northernmost) GW hotspot between 27.5-52.5°N (62.5-87.5°N)
- Enhanced GW parameters: **zonal GW drag:** $-10 \text{ ms}^{-1} \text{ day}^{-1}$
meridional GW drag: $-0.1 \text{ ms}^{-1} \text{ day}^{-1}$
Heating: 0.05 K day^{-1}

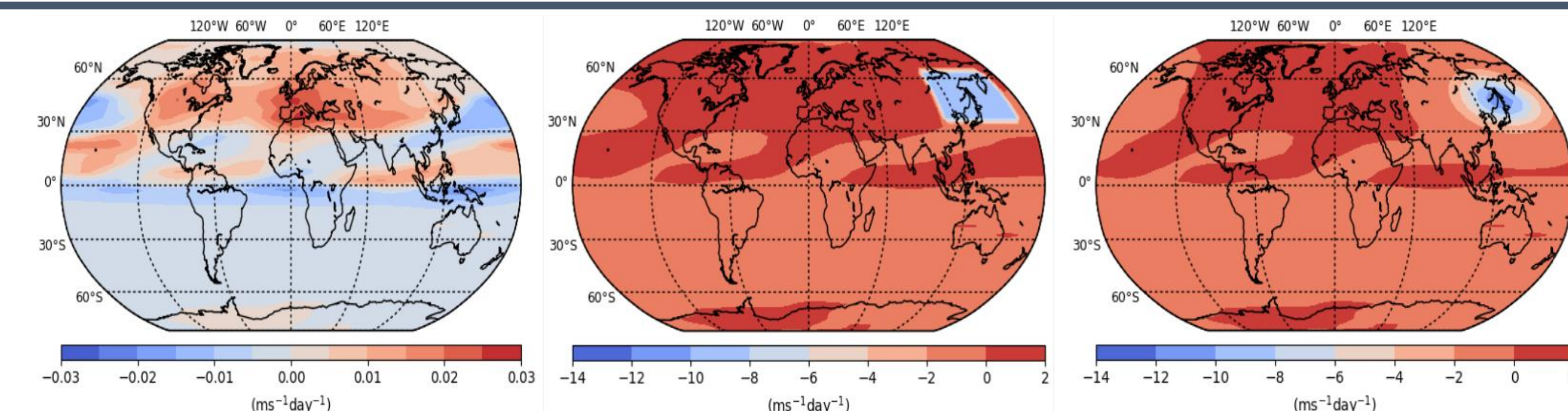


Fig. 4: Zonal GW drag ($\text{ms}^{-1} \text{ day}^{-1}$) at 26.9 km for the reference (left) and the H3 hotspot simulation as box (middle) and as Gaussian distribution (right) for the last 30 days of analysis. Note the different scaling on the left panel.

Results: Background and stationary Planetary Waves

- H3 (37.5-62.5°N) GW hotspot, which is half located in the easterlies (not acting against the zonal mean zonal wind) as well as in the westerlies leads to:
 - a **weakening of the Aleutian high pressure system**,
 - a **displacement of the polar vortex** towards Canada (see Fig. 5).
- Changes in Background conditions:**
 - decreasing zonal mean zonal wind at middle to high latitudes,
 - heating of the lower stratosphere,
 - increasing geopotential height.
- In case of the H7 (57.5-82.5°N) GW hotspot the polar vortex is less disturbed so that the **differences are much smaller**.
- Decreasing zonal wind SPW 1 amplitudes** at lower to middle latitudes between 20 and 60km, because less SPW 1 are propagating upwards, which can be seen by means of the **decreasing Eliassen-Palm (EP) flux**.
- GW hotspot is leading to a **negative refractive index**, which suppresses the propagation of SPW 1 at midlatitudes.
- A reversed meridional potential vorticity gradient indicates **baroclinic instability generating SPW 1 in the polar region** corresponding to the strong positive EP divergence.

- Preconditioning of the polar vortex -

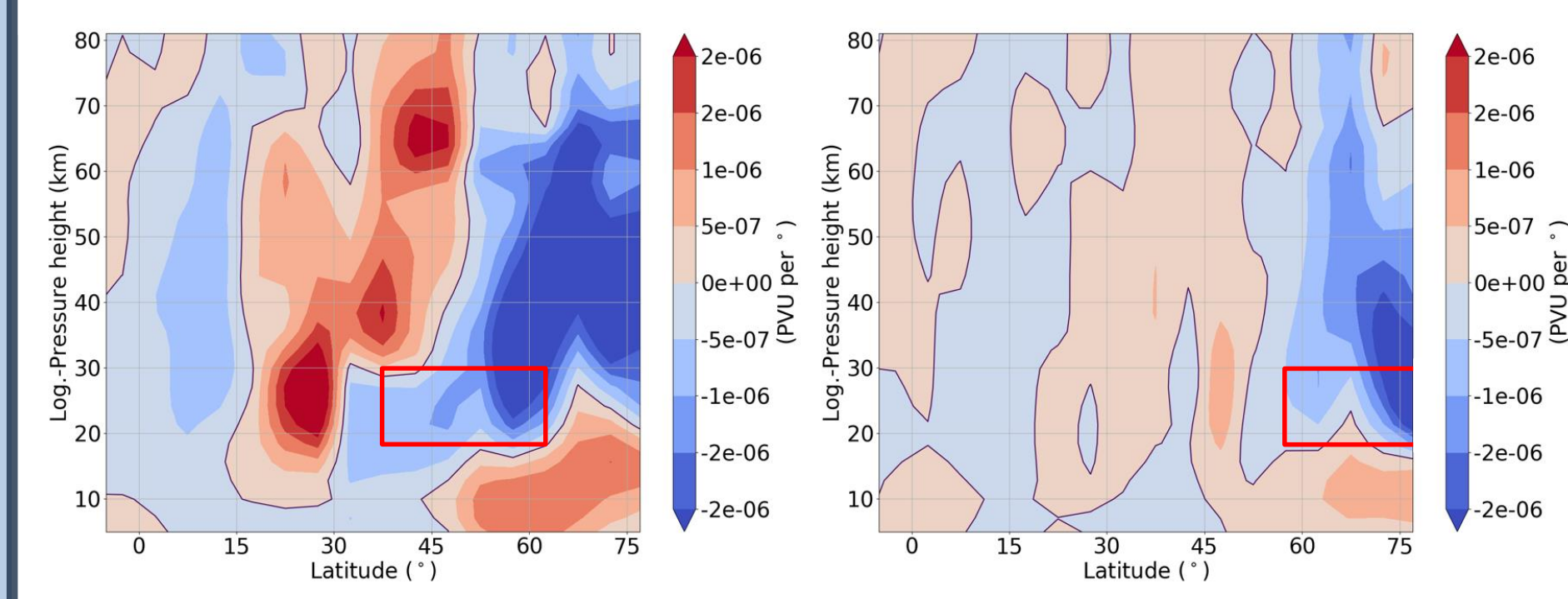


Fig. 9: Meridional potential vorticity gradient difference between the H3 (left panel), H7 (right panel) and the Ref simulation representing the last 30 days of the simulations. The positions of the H3 and H7 GW hotspot is represented by the red boxes.

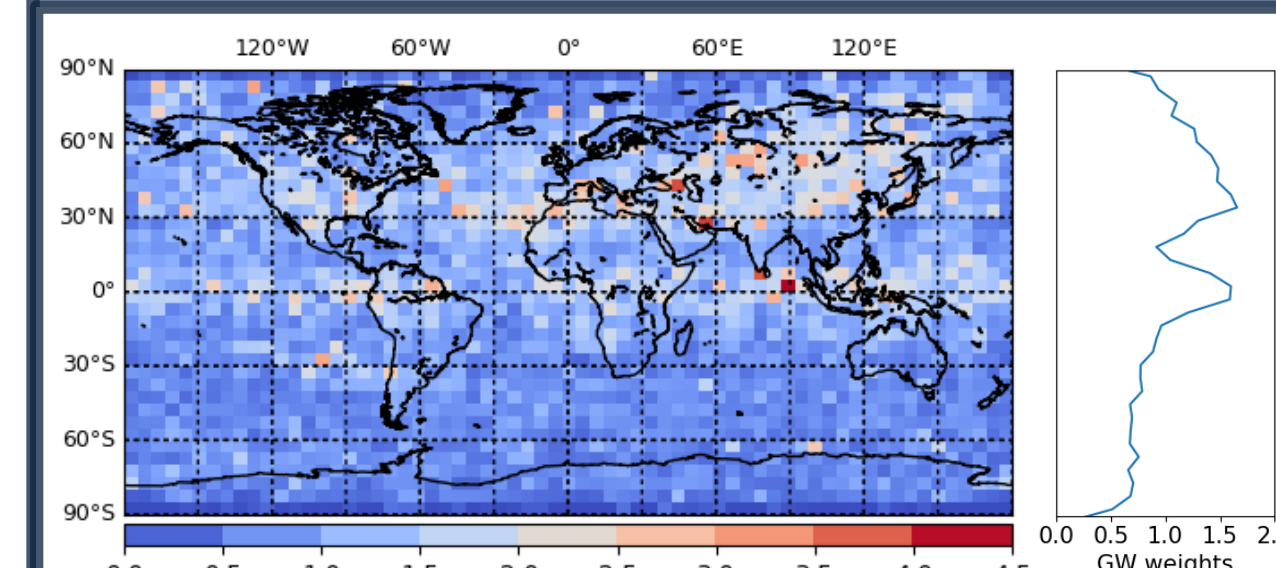


Fig. 2: Global GW weights derived from E_{pot} data and the resulting zonal mean GW weights for MUAM (right, blue contour line).

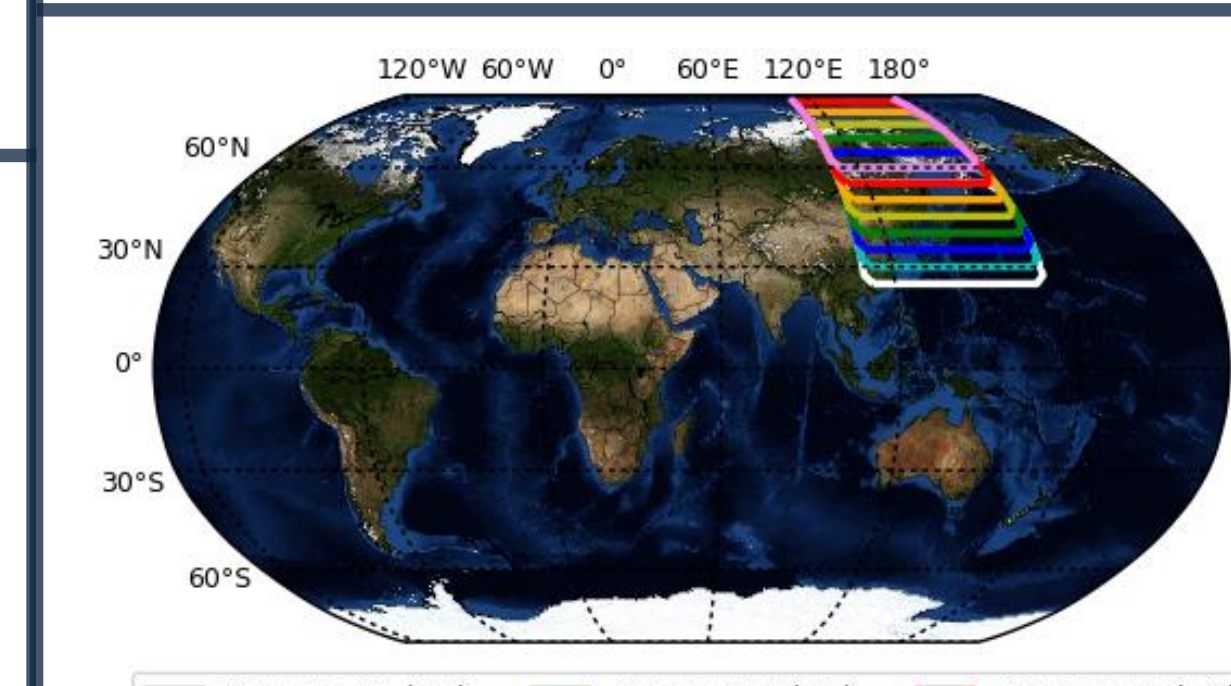


Fig. 3: Positions of the artificial GW hotspots, which have been analyzed in this sensitivity study.

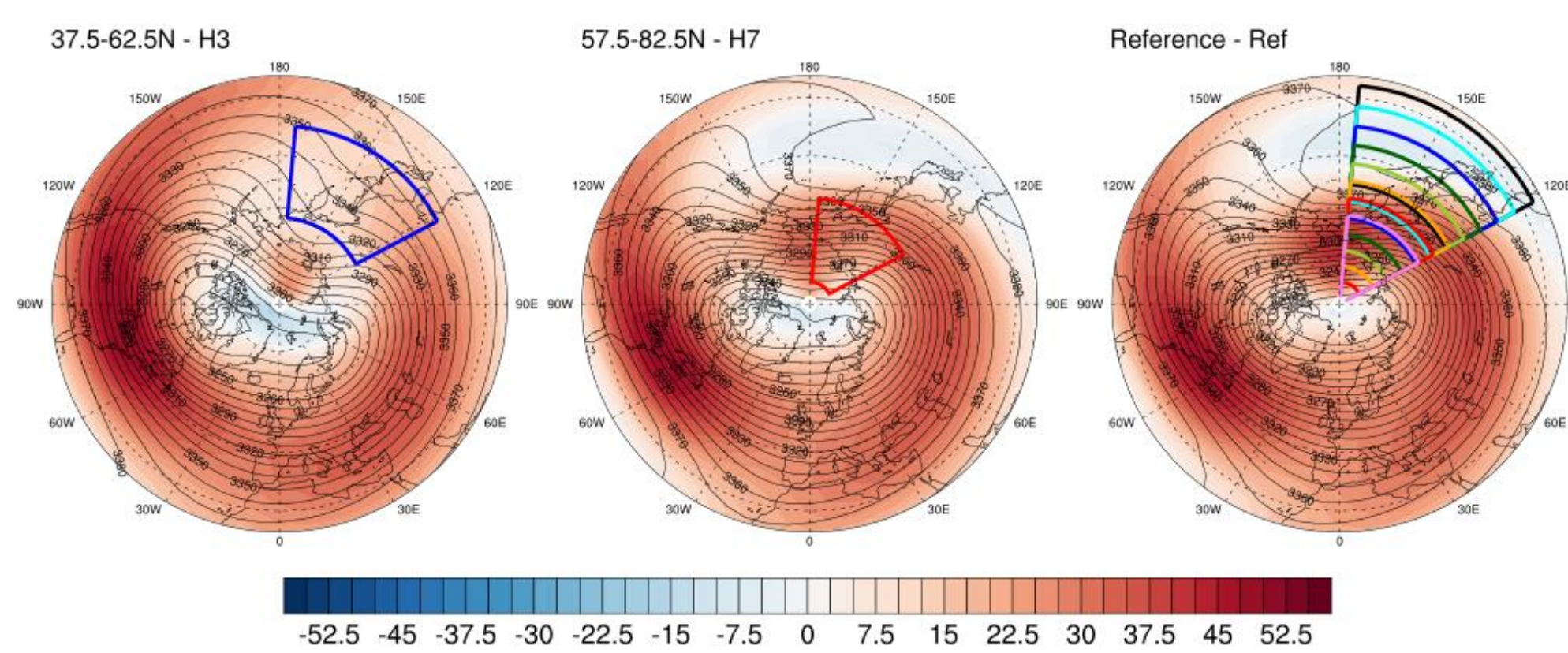


Fig. 5: Zonal wind (ms^{-1}) in colour and geopotential height (gpdam) as contour lines northward of 25°N at 35 km for the H3 (left panel), H7 (middle panel) and the Ref simulation (right panel) representing the last 30 days of analysis. The boxes illustrate the position of each GW hotspot (H1 - H8 (in violet)). The blue (left and right panel) (red (middle and right panel)) box refers to the H3 (H7) simulation.

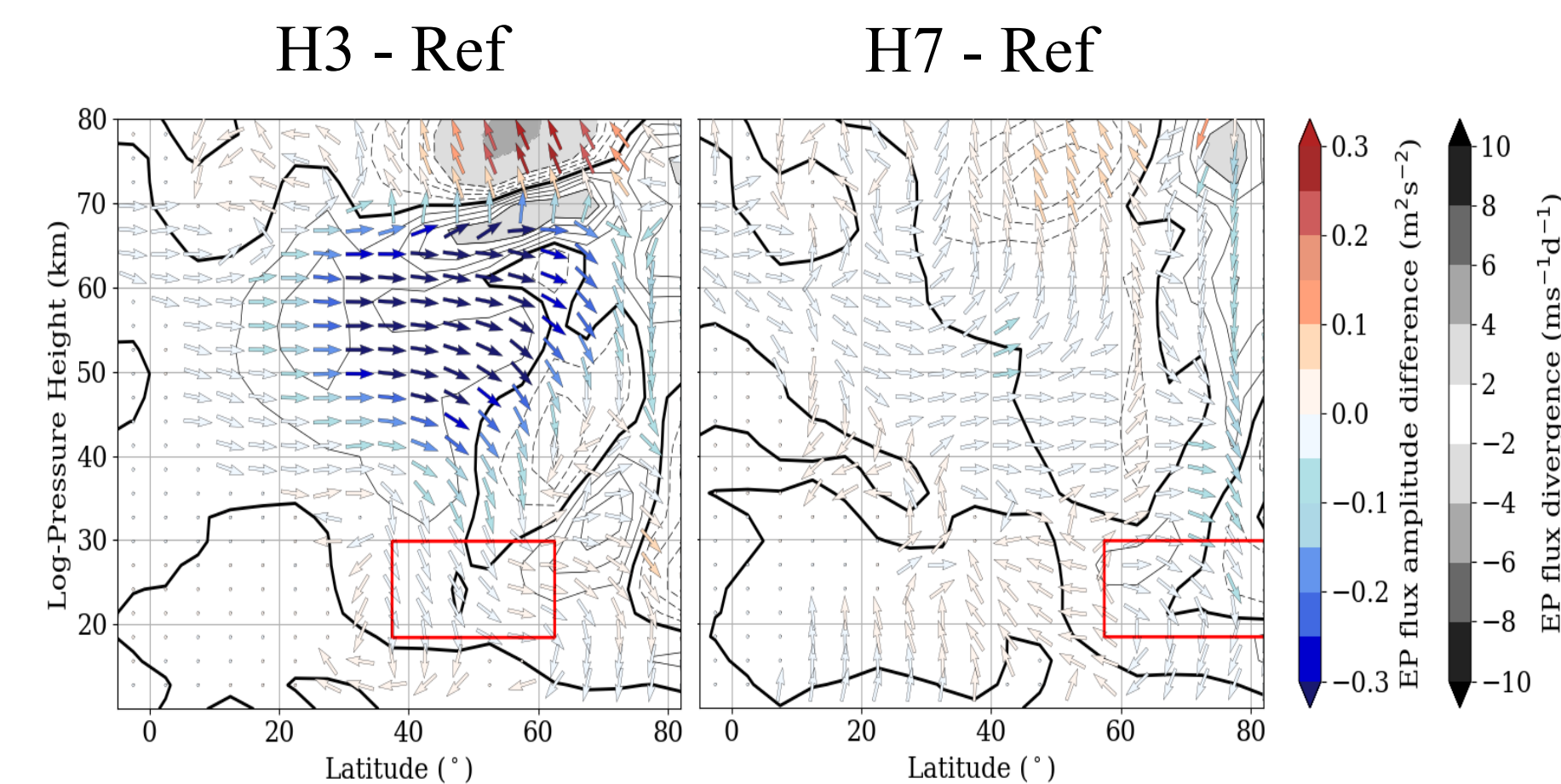


Fig. 7: Zonal mean EP flux (arrows) and divergence (isolines and shaded areas, dashed lines show negative values) of SPW 1. Shown is the difference between all H3 (left)/H7 (right) simulations and the Ref simulation.

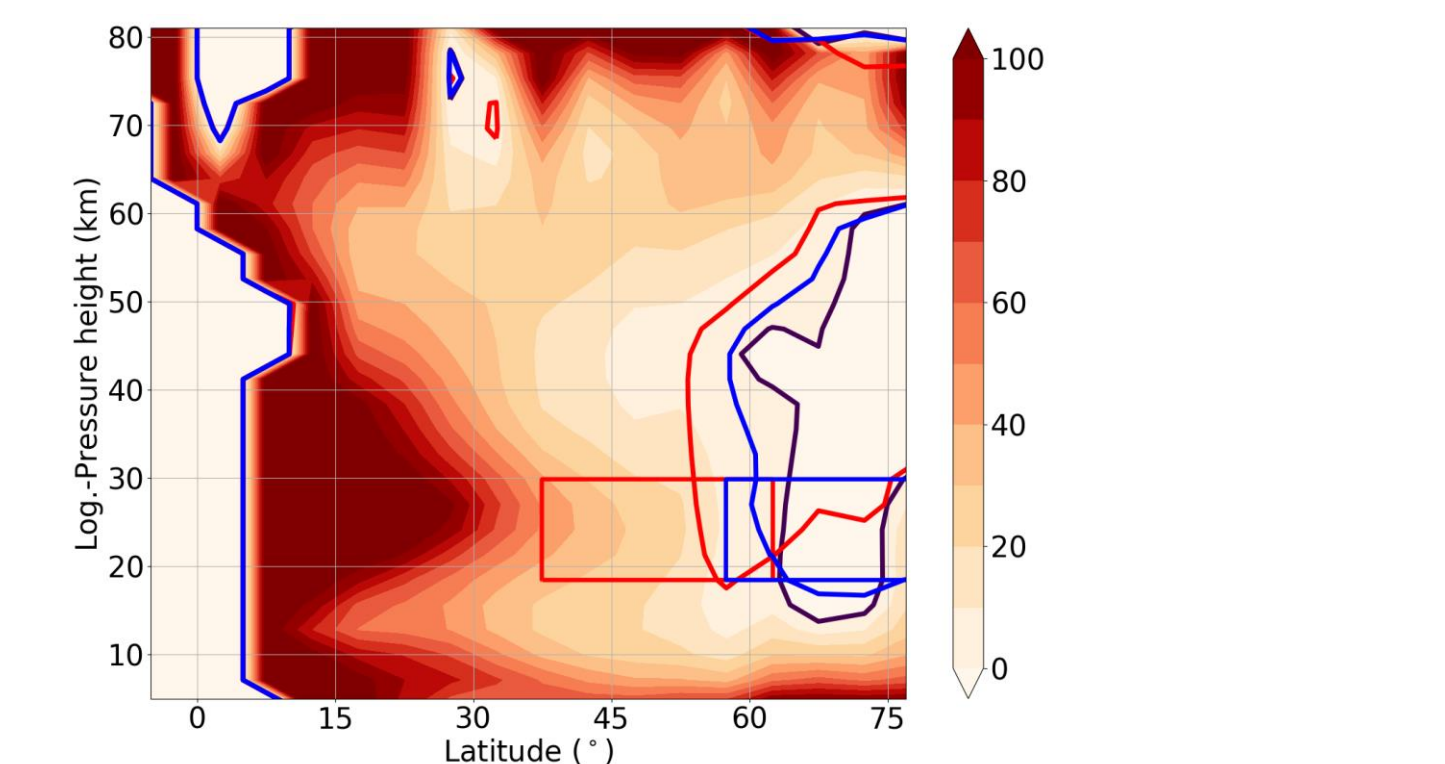


Fig. 8: Refractive index for SPW 1 for the Ref simulation (right panel) with a thicker zero line colored in violet. The position of the H3 (H7) GW hotspot and the respective zero line is represented by the red (blue) line.

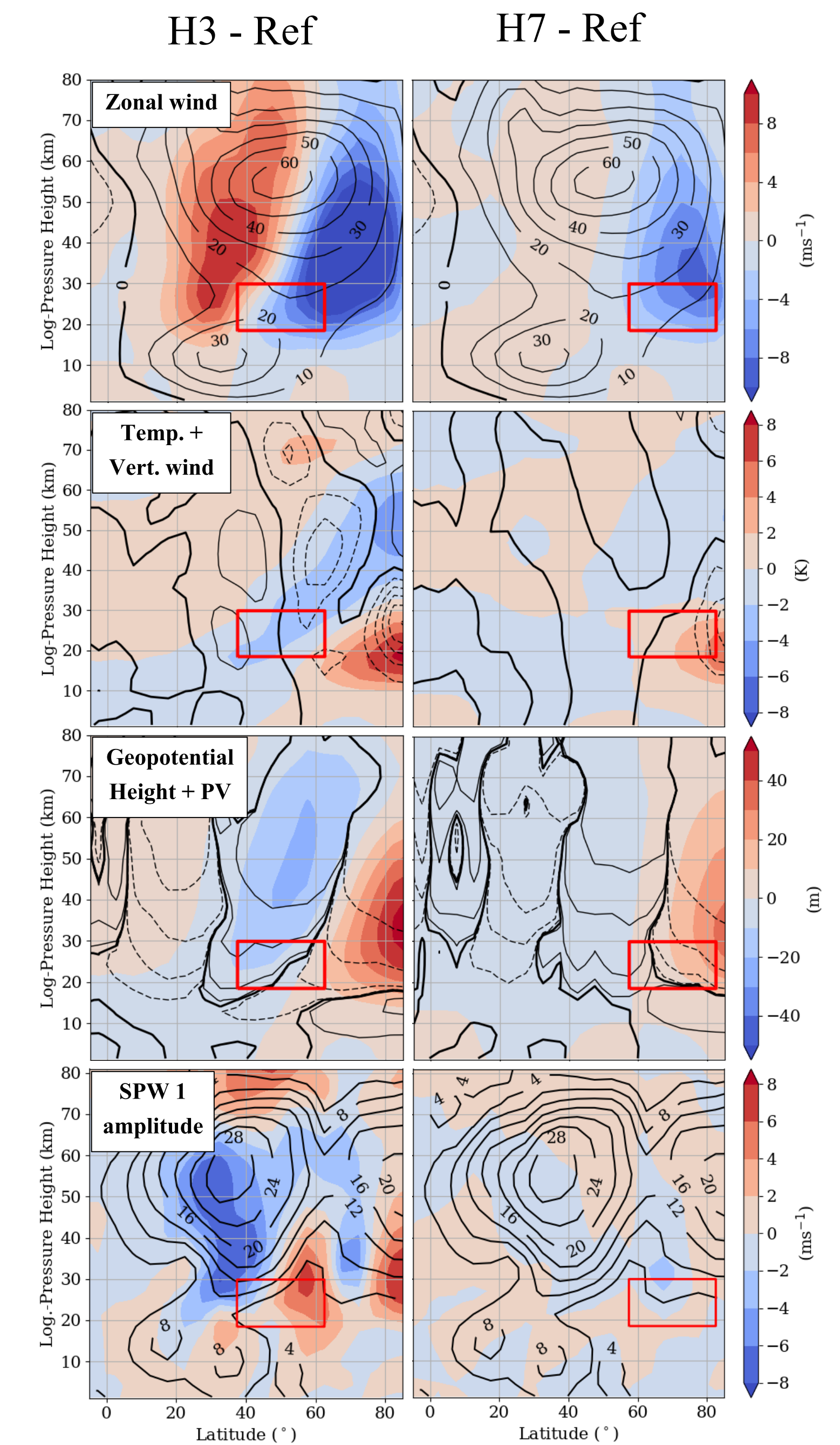


Fig. 6: Zonal wind (1st row), temperature (2nd row) geopotential height (3rd row) and zonal wind SPW 1 amplitude (4th row) differences of the H3 (left) and H7 (right) GW hotspot also including zonal mean zonal wind of the Ref simulation (contour lines in zonal wind plot), vertical wind differences (contour lines in temperature plot starting with $\pm 0.0005 \text{ ms}^{-1}$ up to $\pm 0.0025 \text{ ms}^{-1}$ with increments of 0.0005 ms^{-1}), potential vorticity differences (contour lines in geopotential height plot) and zonal wind SPW 1 amplitude of the Ref simulation (contour lines in SPW 1 amplitude plot).

Results: Shape of the forcing

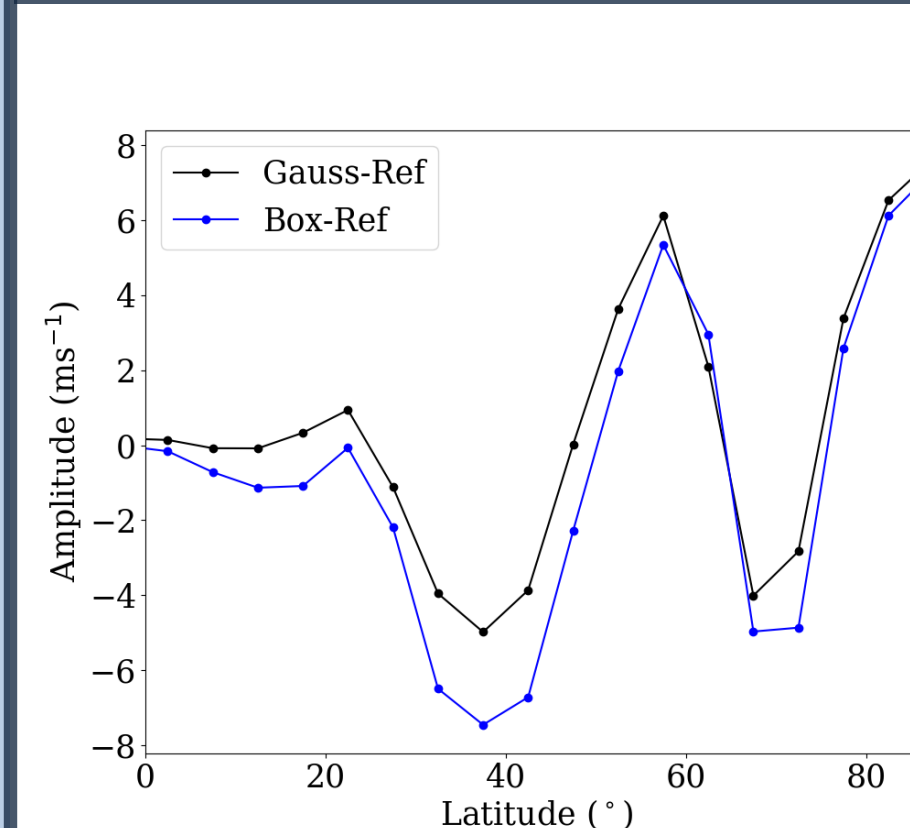


Fig. 10: SPW 1 amplitude as difference between the H3 and the Ref simulation (blue line) and the Gauss distribution and the Ref simulation (black line) at 35 km for the last 30 days extracted from the zonal wind.

- References** Albers, J. R. and Birner, T.: Vortex Preconditioning due to Planetary and Gravity Waves prior to Sudden Stratospheric Warnings, *J. Atmos. Sci.*, 71, 4028-4054, <https://doi.org/10.1175/JAS-D-14-0026.1>, 2014.
- Lilienthal, F., Jacobi, Ch., Schmidt, T., de la Torre, A. and Alexander, P.: 2017, On the influence of zonal gravity wave distributions on the Southern Hemisphere winter circulation, *Ann. Geophys.*, 35, 785-798, <https://doi.org/10.5194/angeo-35-785-2017>.
- Šácha, P., Kuchar, A., Jacobi, C., and Pišoft, P.: Enhanced 5 internal gravity wave activity and breaking over the Northeastern Pacific / Eastern Asian region, *Atmos. Chem. Phys.*, 15, 13 097-13 112, <https://doi.org/10.5194/acp-15-13097-2015>, 2015.
- Samtleben, N., Jacobi, C., Pišoft, P., Šácha, P., and Kuchar, A.: Effect of latitudinally displaced gravity wave forcing in the lower stratosphere on the polar vortex stability, *Ann. Geophys. Discuss.*, <https://doi.org/10.5194/angeo-2019-15>, in review, 2019.
- Acknowledgements** This study has been supported by Deutsche Forschungsgemeinschaft (DFG) under the grant JA836/32-1. ECMWF reanalysis data are provided by apps.ecmwf.int/datasets/data/.